

# High-Quality $\alpha$ -MnSe Nanostructures with Superior Lithium Storage Properties

*Na Li<sup>‡</sup>, Yi Zhang<sup>‡</sup>, Hongyang Zhao, Zhengqing Liu, Xinyu Zhang and Yaping Du\**

**Chemicals.** Oleylamine (OM, 70%, Sigma-Aldrich), oleic acid (OA, 90%, Sigma-Aldrich), 1-octadecene (ODE, >90%, Sigma-Aldrich), decanoic acid (>90%, Sigma-Aldrich), 1-dodecanethiol (1-DDT,  $\geq$ 98%, Sigma-Aldrich),  $\text{Mn}(\text{CH}_3\text{COO})_2 \cdot 4\text{H}_2\text{O}$  (99%, Alfa Aesar), Se (>99.5%, Alfa Aesar),  $\text{Mn}(\text{C}_5\text{H}_7\text{O}_2)_2$  (99%, Alfa Aesar), sodium dodecyl sulfonate (SDS) (99%, Alfa Aesar),  $\text{NH}_4\text{VO}_3$  (99%, Alfa Aesar), oxalic acid (99%, Alfa Aesar), LiAc (99%, Alfa Aesar) and  $\text{NH}_4\text{H}_2\text{PO}_4$  (99%, Alfa Aesar), ethanol (AR) and cyclohexane (AR) were used as received without further purification.

**Characterizations:** TEM images were acquired by a Hitachi HT-7700 transmission electron microscope (TEM, Japan) operating at 100 kV. High-resolution TEM (HRTEM) micrographs were obtained with a Philips Tecnai F20 FEG-TEM (The USA) operated at 200 kV. Samples for TEM analysis were prepared by drying a drop of cyclohexane solution containing the nanomaterials on the surface of a carbon-coated copper grid. The XRD patterns were obtained using a Rigaku D/MAX-RB with monochromatized Cu K $\alpha$  radiation ( $\lambda=1.5418 \text{ \AA}$ ) in the  $2\theta$  ranging from  $10^\circ$  to  $80^\circ$ . X-ray photoelectron spectra (XPS) were conducted using a PHI Quantera SXM instrument equipped with an Al X-ray excitation source (1486.6 eV). Binding

energies (BEs) are referenced to the C 1s of carbon contaminants at 284.6 eV. The electrochemical performances of samples were carried out on a CHI660D electrochemistry workstation and Land Battery Measurement System at room temperature.

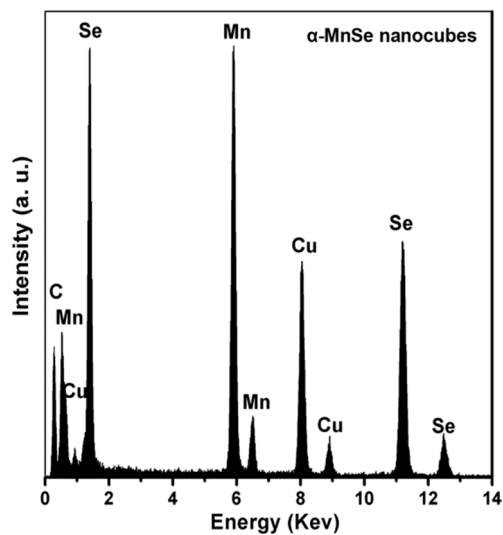


**Figure S1.** The energy dispersive X-ray analysis (EDAX) spectrum of **MS1**, and the Cu signals in peaks were from the copper grid.

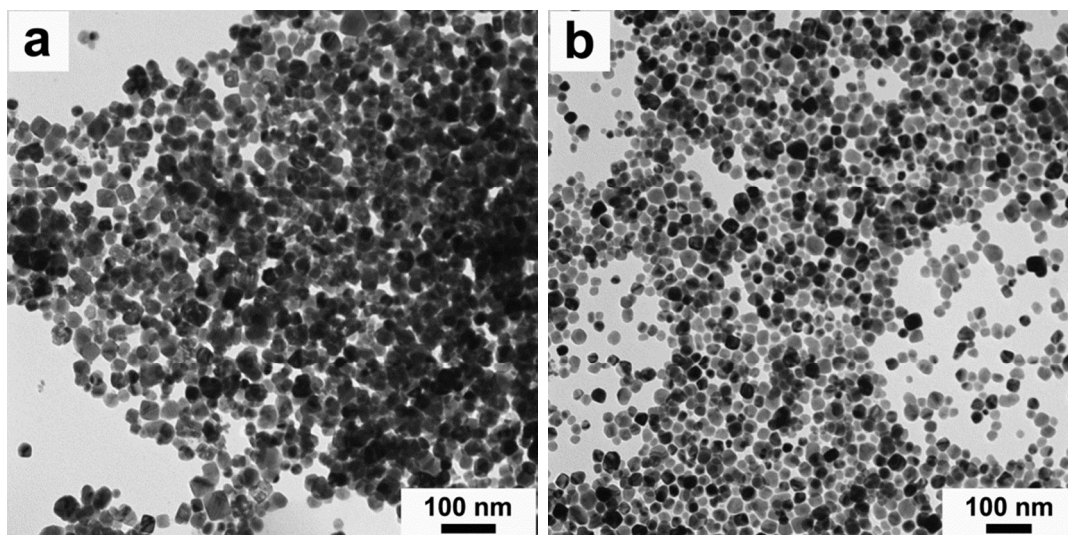


**Figure S2.** TEM images of the as-obtained **MS1** product *via* reacting different mole ratios of two precursors in OM (26.6 mmol), OA (3.4 mmol) and ODE (10 mmol) at 220 °C for 2h: (a)  $\text{Mn}(\text{CH}_3\text{COO})_2 \cdot 4\text{H}_2\text{O}$  (1.0 mmol)/Se (0.5 mmol) = 2/1; (b)  $\text{Mn}(\text{CH}_3\text{COO})_2 \cdot 4\text{H}_2\text{O}$  (0.5 mmol)/Se (1.0 mmol) = 1/2.

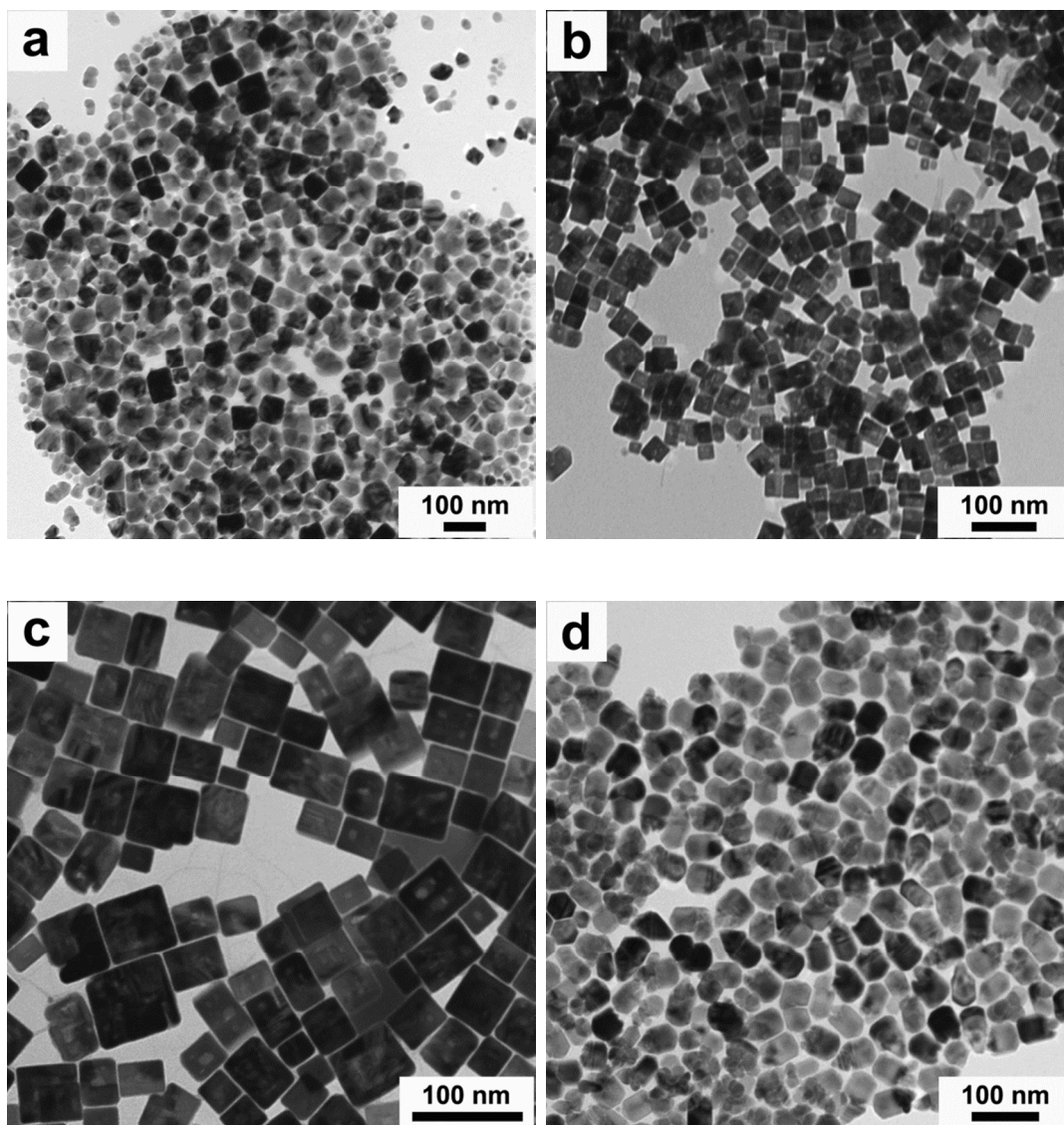


**Figure S3.** TEM images of the as-obtained **MS1** product *via* reacting 0.5 mmol of  $\text{Mn}(\text{CH}_3\text{COO})_2 \cdot 4\text{H}_2\text{O}$  and 0.5 mmol of Se in different ratio of solvent mixture (OM/OA/ODE) at 220 °C for 2 h: (a) OM/OA/ODE = 30.0 mmol/ 0 mmol/ 10.0 mmol, (b) OM/OA/ODE= 28.2 mmol/ 1.8 mmol/ 10.0 mmol, (c) OM /OA /ODE = 27.7 mmol/ 2.3 mmol/ 10.0 mmol, (d) OM/OA /ODE = 25.7 mmol/ 4.3 mmol/ 10.0 mmol.

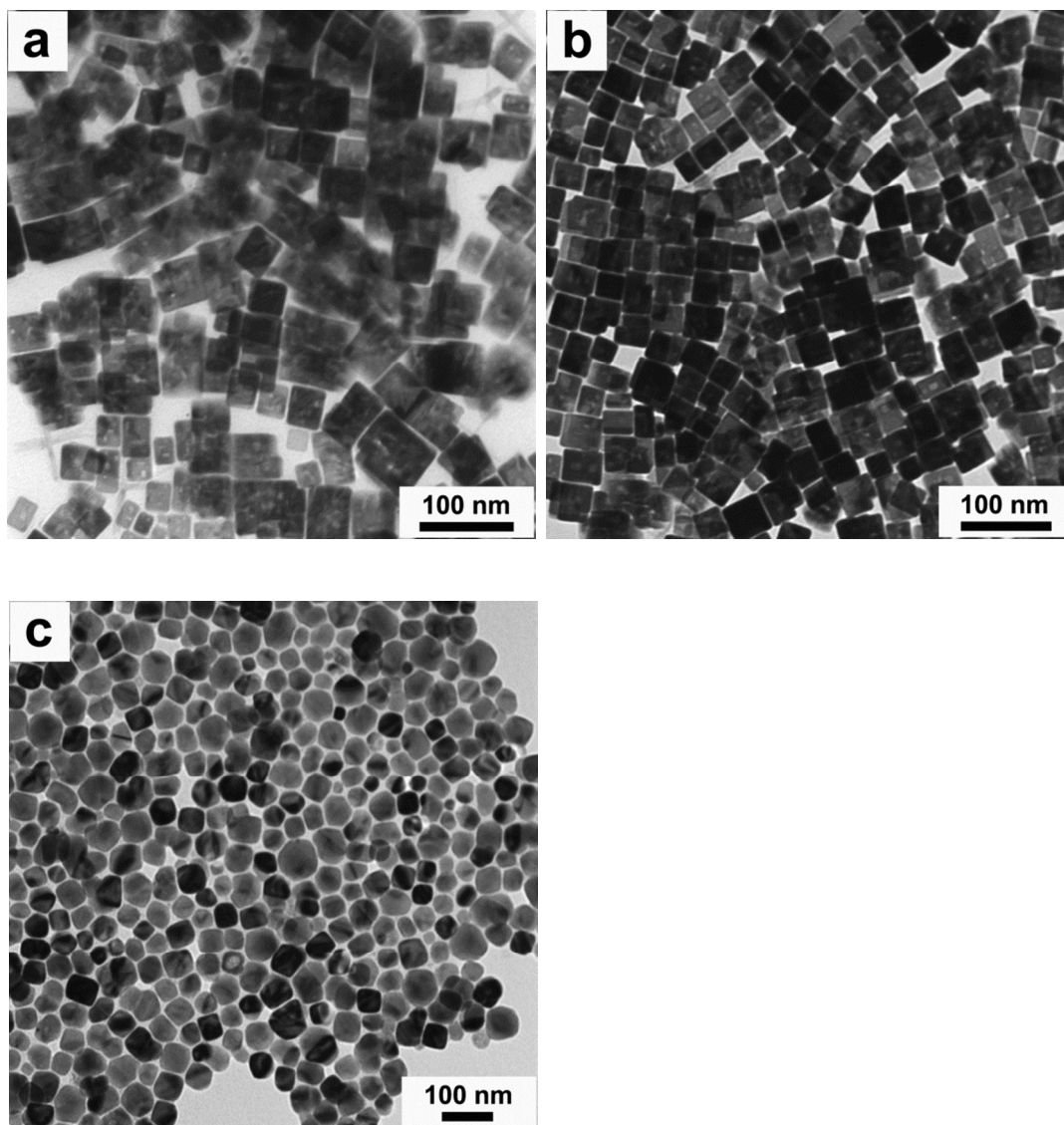


**Figure S4.** TEM images of the as-obtained **MS1** product *via* reacting 0.5 mmol of  $\text{Mn}(\text{CH}_3\text{COO})_2 \cdot 4\text{H}_2\text{O}$  and 0.5 mmol of Se in OM (26.6 mmol), OA (3.4 mmol) and ODE (10.0 mmol) at different temperatures for 2 h: (a) 200 °C, (b) 210 °C, (c) 240 °C.

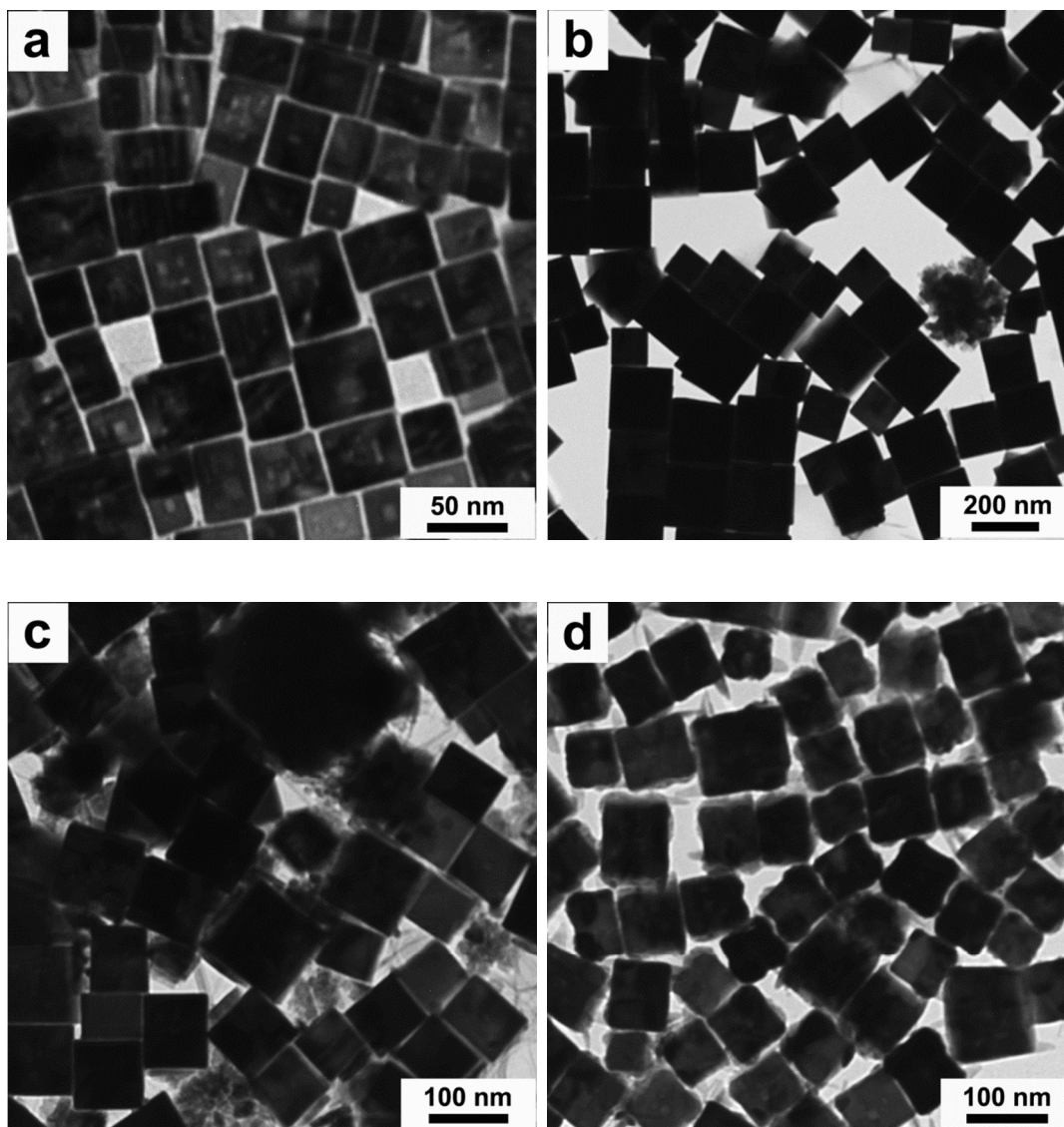


**Figure S5.** TEM images of the as-obtained MS1 product *via* reacting 0.5 mmol of  $\text{Mn}(\text{CH}_3\text{COO})_2 \cdot 4\text{H}_2\text{O}$  and 0.5 mmol of Se in OM (26.6 mmol), OA (3.4 mmol) and ODE (10.0 mmol) at 220 °C for different reaction time: (a) 30 min, (b) 4 h, (c) 8 h, (d) 18 h.

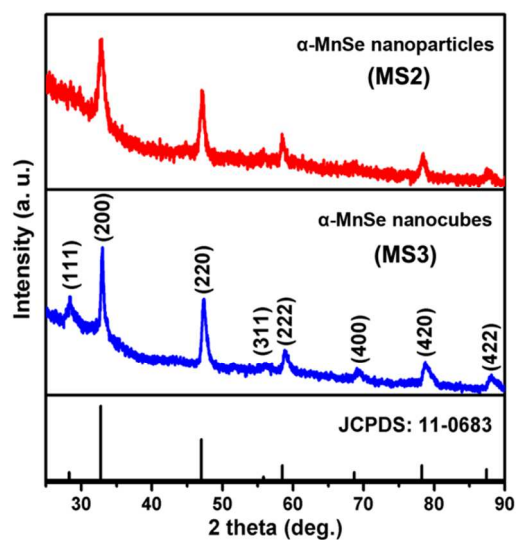


Figure S6. XRD patterns of as-obtained MS2 and MS3 samples.

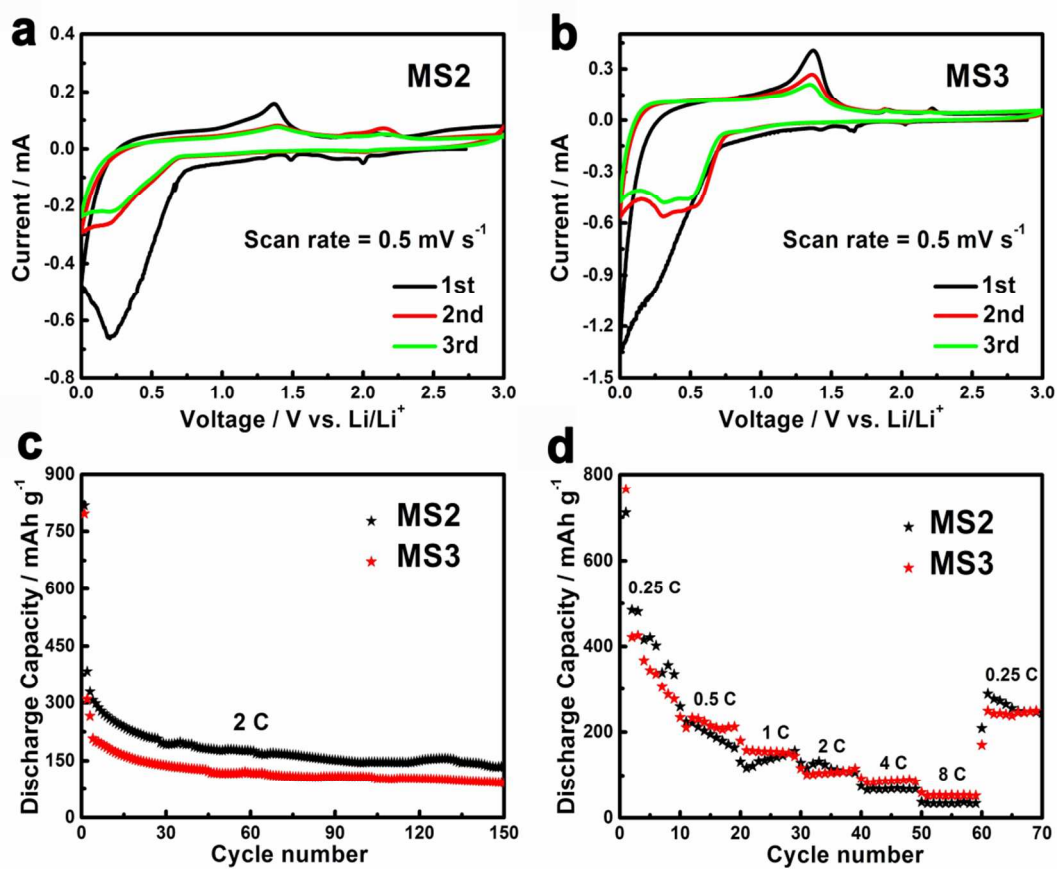
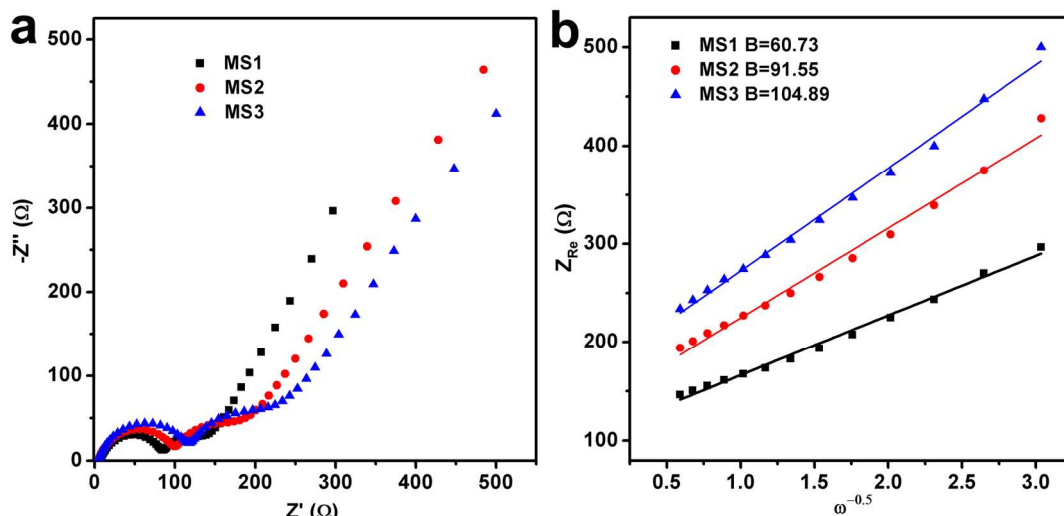


Figure S7. The electrochemical performance of as-obtained MS2 and MS3 samples.



**Figure S8.** (a) EIS Nyquist plots of **MS1**, **MS2**, **MS3** after 50 cycles. (b) The value of  $\omega^{-0.5}$  was the slope of linear fit of the curve. The three coin cells were cycled for 50 cycles and then fully discharged. As shown in Figure S8a, three samples showed two semi-circles, indicating the charge transfer process in the samples and the formation of SEI layer. The linear part of the Nyquist plot suggested the mass transfer process. The diameter of the first semi-circle of the MS1 sample was the smallest among the three samples in Nyquist plot, demonstrating the MS1 sample has the smallest charge-transfer impedance. The linear part in the low frequency region of Nyquist plot represented the mass transfer process. The lithium ion diffusion coefficient  $D$  was related with  $1/(2B)$ , where  $B$  was the Warburg coefficient. The value of  $B$  was the slope of linear fit of the curve in Figure S8b, where  $Z_{Re}$  was the real part of impedance, and  $\omega$  was the angular frequency. It can be calculated that MS1 sample has the smallest  $B$  value, indicating MS1 sample has the largest lithium ion diffusion efficiency. According to the above analysis, we thought the sample MS1 was the optimized sample for lithium ion battery anode material in current work.